



**HAL**  
open science

## **Adaptive thermostability of light-harvesting complexes in marine picocyanobacteria**

Justine Pittera, Frédéric Partensky, Christophe Six

► **To cite this version:**

Justine Pittera, Frédéric Partensky, Christophe Six. Adaptive thermostability of light-harvesting complexes in marine picocyanobacteria. *The International Society of Microbiological Ecology Journal*, 2017, 11 (1), pp.112 - 124. <10.1038/ismej.2016.102>. <hal-01509871>

**HAL Id: hal-01509871**

**<https://hal.sorbonne-universite.fr/hal-01509871v1>**

Submitted on 18 Apr 2017

**HAL** is a multi-disciplinary open access archive for the deposit and dissemination of scientific research documents, whether they are published or not. The documents may come from teaching and research institutions in France or abroad, or from public or private research centers.

L'archive ouverte pluridisciplinaire **HAL**, est destinée au dépôt et à la diffusion de documents scientifiques de niveau recherche, publiés ou non, émanant des établissements d'enseignement et de recherche français ou étrangers, des laboratoires publics ou privés.



HAL Authorization

2 **Adaptive thermostability of light-harvesting complexes in marine**  
3 **picocyanobacteria**

4 Justine Pittera<sup>1,2</sup>, Frédéric Partensky<sup>1,2</sup> & Christophe Six<sup>1,2</sup>

5

6 <sup>1</sup>Sorbonne Universités, Université Pierre and Marie Curie (Paris 06), UMR 7144, Marine Phototrophic  
7 Prokaryotes (MaPP) Team, Station Biologique, Place Georges Teissier, CS 90074, 29688 Roscoff  
8 cedex, France.

9 <sup>2</sup>Centre National de la Recherche Scientifique, UMR 7144, Marine Plankton Group, Station  
10 Biologique, CS 90074, 29688 Roscoff cedex, France.

11

12 **Running title:** Phycobilisome thermoadaptation in *Synechococcus*

13 **Key words:** temperature, picocyanobacteria, marine *Synechococcus*, phycobilisome,  
14 phycobiliprotein, protein thermostability, ecotype

15 **Subject category:** Microbial ecology and functional diversity of natural habitats

16

17 **To whom correspondence should be addressed:** Christophe Six

18 Station Biologique de Roscoff,

19 CS 90074,

20 29688 Roscoff, France.

21 Phone: +33 2 98292534

22 Email: [christophe.six@sb-roscoff.fr](mailto:christophe.six@sb-roscoff.fr)

23

24 We certify that there is no conflict of interest with any financial organization regarding the material  
25 discussed in this manuscript.

26 **Abstract**

27 Marine *Synechococcus* play a key role in global oceanic primary productivity. Their wide latitudinal  
28 distribution has been attributed to the occurrence of lineages adapted to distinct thermal niches, but  
29 the physiological and molecular bases of this ecotypic differentiation remain largely unknown. By  
30 comparing six strains isolated from different latitudes, we showed that the thermostability of their  
31 light-harvesting complexes, called phycobilisomes, varied according to the average sea surface  
32 temperature at strain isolation site. Comparative analyses of thermal unfolding curves of the three  
33 phycobiliproteins constituting phycobilisome rods suggested that the differences in thermostability  
34 observed on whole phycobilisomes relied on the distinct molecular flexibility and stability of their  
35 individual components. Phycocyanin was the least thermostable of all rod phycobiliproteins,  
36 constituting a fragility point of the phycobilisome under heat stress. Amino acid composition  
37 analyses and structural homology modeling notably revealed the occurrence of two amino acid  
38 substitutions, which might play a role in the observed differential thermotolerance of this  
39 phycobiliprotein among temperature ecotypes. We hypothesize that marine *Synechococcus*  
40 ancestors occurred first in warm niches and that during the colonization of cold, high latitude  
41 thermal niches, their descendants have increased the molecular flexibility of phycobiliproteins to  
42 maintain optimal light absorption capacities, this phenomenon likely resulting in a decreased stability  
43 of these proteins. This apparent thermoadaptability of marine *Synechococcus* has most probably  
44 contributed to the remarkable ubiquity of these picocyanobacteria in the ocean.

45

## 46 **Introduction**

47 Temperature is an environmental factor that greatly impacts the distribution of living forms on  
48 our planet. Temperature varies widely over the course of the day, seasons as well as across latitudes  
49 and therefore constitutes a major ecological constraint on the physiology of organisms and hence on  
50 the functioning of ecosystems. In particular, temperature is one of the main factors controlling  
51 inorganic carbon fixation, a process which in the oceans is prevalently ensured by phytoplanktonic  
52 cells (Behrenfeld *et al.*, 2006; Falkowski, 1994). Among these, *Prochlorococcus* and *Synechococcus*,  
53 two highly abundant picocyanobacteria (< 2  $\mu\text{m}$ ), are thought to be responsible for up to 25% of the  
54 global net oceanic primary production (Flombaum *et al.*, 2013; Partensky *et al.*, 1999). While  
55 *Prochlorococcus* is restricted to the 40 °S – 45 °N latitudinal band, *Synechococcus* occurs from the  
56 equator to polar circles (Huang *et al.*, 2012; Neuer, 1992; Zwirgmaier *et al.*, 2008), suggesting that  
57 this ubiquitous picocyanobacterium has developed efficient adaptive strategies to cope with natural  
58 temperature variations (Mackey *et al.*, 2013; Pittera *et al.*, 2014).

59 Phylogenetic studies using various markers have evidenced the large genetic microdiversity  
60 occurring within the *Synechococcus* genus (Ahlgren & Rocap, 2012; Fuller *et al.*, 2003). For instance,  
61 based on the high resolution *petB* marker, about 15 clades and 28 subclades (Mazard *et al.*, 2012)  
62 have been delineated within the main radiation, called subcluster 5.1 (Herdman *et al.*, 2001). Basin-  
63 scale phylogeographical studies have shown that the most prevalent marine *Synechococcus* lineages,  
64 *i.e.* clades I to IV, occupy distinct ecological niches (Sohm *et al.*, 2015; Zwirgmaier *et al.*, 2008).  
65 Clades I and IV are confined to nutrient-rich, cold or temperate waters at high latitude (> 30°N/S),  
66 whereas clades II and III preferentially thrive in warm waters, with the former being prevalent in  
67 subtropical and tropical open ocean and the latter dominating in the eastern Mediterranean Sea  
68 (Farrant *et al.*, 2016; Mella-Flores *et al.*, 2011; Sohm *et al.*, 2015).

69 Pittera *et al.* (2014) have evidenced a correspondence between the thermophysiology of  
70 *Synechococcus* clades I and II and their respective thermal niches. Indeed, members of these lineages  
71 were shown to exhibit thermal *preferenda* (*i.e.*, temperature growth ranges and growth maxima)

72 consistent with the seawater temperature at their isolation site, as well as a differential sensitivity to  
73 thermal stress. These genetically defined lineages, physiologically adapted to specific thermal niches,  
74 therefore correspond to different ‘temperature ecotypes’ (or ‘thermotypes’), a concept previously  
75 defined for *Prochlorococcus* clades HLI and HLII, which preferentially thrive in cool temperate waters  
76 and warm subtropical waters, respectively, a discrepancy also explained by the distinct growth  
77 temperature characteristics of representative isolates (Johnson *et al.*, 2006; Zinser *et al.*, 2007).  
78 Although other factors such as the macronutrients can be important sources of diversification within  
79 the marine *Synechococcus* radiation, recent field studies have demonstrated that temperature is one  
80 of the main factors explaining the variability of the genotypic composition of marine *Synechococcus*  
81 assemblages, with different thermotypes forming well-defined populations in distinct latitudinal  
82 bands at oceanic basin scales (Farrant *et al.*, 2016; Sohm *et al.*, 2015).

83 Pittera *et al.* (2014) also showed that during thermal stress experiments the capacity of the  
84 temperature ecotypes to acclimate and endure temperature variations notably relies on their ability  
85 to optimize the functionality of their photosystem II (PSII) at different temperatures. This  
86 macromolecular complex is indeed known to be a particularly temperature responsive component of  
87 the photosynthetic machinery (Murata *et al.*, 2007). Like in red algae, the major PSII light-harvesting  
88 antenna of *Synechococcus* is a giant, water soluble pigment-protein complex, the phycobilisome  
89 (PBS). This macrocomplex, composed of a central core surrounded by six rods, is made of  
90 phycobiliproteins (PBP), themselves composed of two subunits ( $\alpha$  and  $\beta$ ) aggregated as hexameric  
91 discs  $(\alpha\beta)_6$ . Different open-chain tetrapyrrolic chromophores, the phycobilins, are bound to the  
92 apoproteins by thioether bonds on cystein residues, and absorb at specific wavelength bands (Glazer,  
93 1985; Glazer, 1989; Sidler, 1994; Six *et al.*, 2007b). Based on their amino acid sequence and  
94 absorption properties, the PBPs have been assigned to distinct classes. The PBS core is always made  
95 of allophycocyanin (APC), which binds the blue chromophore phycocyanobilin (PCB,  $A_{\max} \sim 620$  nm).  
96 In marine *Synechococcus*, the basal part of PBS rods is composed of phycocyanin (PC) that most often  
97 binds PCB and phycoerythrobilin (PEB,  $A_{\max} \sim 550$  nm), usually at a molar ratio of 1:2 (Ong & Glazer

98 1987; Six *et al.*, 2007b; but see also Blot *et al.*, 2009). The distal part of the rods is generally made of  
99 two types of phycoerythrins, PEI and PEII, which display different combinations of PEB and  
100 phycourobilin (PUB,  $A_{\max} \sim 495$  nm), depending on the strain (Humily *et al.*, 2013; Ong & Glazer,  
101 1991; Sidler, 1994). The whole PBS structure is further stabilized by a set of linker polypeptides  
102 (Glazer, 1984). The design of the complex induces a directional transfer of excitation energy from the  
103 rod periphery to the PBS core and *in fine* to reaction centers (Glazer, 1989). The efficiency of the  
104 energy transfer in the PBS may depend on environmental factors, such as incident photon flux or  
105 osmotic pressure, and can be monitored by measuring energy leaks, emitted as fluorescence, for  
106 each PBP (see *e.g.* Ke, 2001; Kupper *et al.*, 2009; Six *et al.*, 2007a).

107 As the PBS constitutes the main entrance gate of light energy into the photosynthetic machinery,  
108 the sustainability of the PBP function is of crucial importance for the cell. In all PBPs, the native  
109 protein molecular environment constrains the phycobilins to a planar conformation that allows  
110 maximal light absorption (Glazer, 1985; MacColl *et al.*, 1980; Scheer & Kufer, 1977). In disordered  
111 proteins, the bilin conformation is no more constrained by the protein environment and tends to  
112 adopt a more cyclic conformation, inducing lower visible light but higher UV absorbance.  
113 Temperature is well known to influence protein conformation and is therefore likely to affect the  
114 function of cofactors such as phycobilins (Bowen *et al.*, 2000). Consequently, during evolution,  
115 different variants of a protein have evolved, with cold environment selecting for more flexible  
116 proteins at the cost of thermostability, whereas warm environments favour stability at the cost of  
117 psychroflexibility (Jaenicke & Böhm, 1998; Szilagyí & Zavodszky, 2000).

118 Here, we combined different approaches to compare the functional thermostability and  
119 molecular flexibility of the photosynthetic antennae of six marine *Synechococcus* strains  
120 representative of different thermotypes and unveiled some of the molecular bases of this adaptation  
121 to temperature.

122

## 123 **Materials and methods**

124 **Biological material and growth conditions**

125 We selected six marine strains isolated at a similar distance from the coast (mesotrophic waters),  
126 along a latitudinal gradient of temperature (Fig. 1, Table 1). The six strains belong to the same PEB-  
127 rich pigment type (3a *sensu* Six *et al.*, 2007b) and have therefore a similar PBS structure and  
128 composition. Clonal *Synechococcus* strains M16.1, RS9907, WH7803, ROS8604, MVIR-16-2 and MVIR-  
129 18-1 (<http://roscoff-culture-collection.org/>) were grown in PCR-S11 culture medium (Rippka *et al.*,  
130 2000) supplemented with 1 mM sodium nitrate, under 80  $\mu\text{mol photons m}^{-2} \text{ s}^{-1}$  white light irradiance  
131 provided by fluorescent tubes (Sylvania Daylight F18W/54-765 T8). Cultures were acclimated for at  
132 least four weeks to a range of temperature (9-35°C) using temperature controlled growth chambers.

133

134 **In vivo fluorescence emission in response to increasing temperature**

135 *Synechococcus* cultures in mid exponential growth phase were placed in a temperature-controlled  
136 water bath at growth temperature in the dark. Temperature was then progressively increased by 3°C  
137 steps of 10 min, up to 46°C. At the end of each temperature level, an *in vivo* fluorescence emission  
138 spectrum was recorded upon excitation at 530 nm using a LS-50B spectrofluorimeter (Perkin Elmer).  
139 The energy transfer between the PBPs was assessed by measuring their relative fluorescence  
140 emission levels, since increases in the relative heights of the PC or PE emission peaks are indicative of  
141 energy leaks. The PE to PC fluorescence emission ratio was then calculated, log-transformed and  
142 plotted against instantaneous temperature by homology with the well-known Arrhenius breaking  
143 temperature plots, allowing us to determine the PBS breaking temperature ( $T_{\text{PBS}}$ ; Dahlhoff *et al.*,  
144 1991; Stillman & Somero, 1996); Fig. S1). For further analyses, the fluorescence emission spectra  
145 were decomposed using the a|e – UV-Vis-IR Spectral software 2.0 ([www.fluortools.com](http://www.fluortools.com)).

146

147 **Phycobiliprotein denaturation curves**

148 Phycobiliprotein purification was carried out using sucrose gradients and isoelectric focusing, as  
149 previously described (Six *et al.*, 2005). PBP structural thermostability was assessed by monitoring

150 phycobilin absorbance and fluorescence along protein thermal unfolding curves (Grimsley *et al.*,  
151 2013), from 30°C to 85°C, with PBP solutions at about 30 nM for PEs ( $2.15 \cdot 10^6 \text{ M}^{-1} \text{ cm}^{-1}$  and  $2.41 \cdot 10^6$   
152  $\text{M}^{-1} \text{ cm}^{-1}$  for at 545 nm PEII and PEI respectively; Glazer & Hixson, 1977; Wyman 1992) and 100 nM  
153 for PC ( $2 \cdot 10^5 \text{ M}^{-1} \text{ cm}^{-1}$  at 620 nm as estimated from Glazer *et al.*, 1973 and Glazer & Hixson, 1975).  
154 Absorption and fluorescence emission spectra were recorded during a progressive temperature  
155 increase, performed by 5°C steps of 5 min each. The fluorescence emission spectra were recorded  
156 upon excitation at 545 nm for PE and 620 nm for PC and the absorbance was monitored at the  
157 wavelength of the acceptor phycobilins, *i.e.* PEB in PEs (~ 545 nm) and PCB in PCs (~ 620 nm; Sidler,  
158 1994). For each PBP, the absorbance values were plotted against instantaneous temperature and  
159 fitted with a sigmoid curve using the following equation:

$$y = b + \frac{a - b}{1 + 10^{(\log T_{50\%})s}}$$

160 where  $a$  is the initial maximal absorption,  $b$  the absorption minimum at 85°C and  $s$  the Hill slope of  
161 the function. The mid-unfolding temperature  $T_{50\%}$ , *i.e.* the temperature at which the protein has lost  
162 half of its absorption capacities, which is related to the molecular flexibility of the protein, was  
163 determined using the Sigma Plot v10 software (Figs. S2 & S3).

164

### 165 ***Analysis of phycobiliprotein sequences and homology modeling***

166 Using GenBank and the Cyanorak interface (<http://application.sb-roscoff.fr/cyanorak/>), we  
167 compiled a database encompassing the sequences of the two subunits of 21 PC, 21 PE-I and 20 PE-II.  
168 Unpublished sequences were deposited in GenBank nucleotide sequence database under accession  
169 numbers mentioned in Table S1. All sequences were aligned using Bioedit 7.2.3 (Hall, 1999) and the  
170 distributions and amino acid frequencies of PC (RpcA and RpcB), PEI (CpeA and CpeB) and PEII (MpeA  
171 and MpeB) subunits were computed using ProtParam Tools (ExPASy, Gasteiger *et al.*, 2005).  
172 Differences in the biochemical parameters of the  $\alpha$ - and  $\beta$ -subunit sequences were tested using the  
173 non-parametric statistical test of Wilcoxon, and differences among clades were tested using Kruskal-  
174 Wallis test. Whether the observed substitutions were conservative or not was assessed using the

175 MAFFT v7 software (Katoh & Standley, 2013). Physicochemical parameters of the PBP were retrieved  
176 using the ProtParam tool and the molecular flexibility was calculated with ProtScale (Gasteiger *et al.*,  
177 2005).

178 The crystal structure of *Spirulina platensis* PC (Padyana *et al.*, 2001; PDB ID: 1HA7) was retrieved  
179 from the Protein Data Bank (Berman *et al.*, 2003) and used as a template for modeling  
180 *Synechococcus* PC. Structural protein models were generated using Phyre<sup>2</sup> (Kelley & Sternberg 2009).  
181 The PCB and PEB structures were retrieved from *Polysiphonia urceolata* (Jiang *et al.*, 2001; PDB ID:  
182 1F99). Models were then visualized and aligned using PyMOL v 1.7.4. *Synechococcus* PC models were  
183 superimposed and the PC structural differences related to amino acid substitutions were compared  
184 between cold- and warm-environment strains.

185

## 186 **Results and discussion**

### 187 ***Marine Synechococcus phycobilisome function optimally in specific thermal ranges***

188 The six *Synechococcus* strains were isolated from different latitudes and thermal niches (Fig. 1).  
189 The temperature range for growth and *preferenda* of five of them were characterized in a previous  
190 study, while those of a sixth one isolated from the Red Sea, RS9907, is reported here (Table 1). Their  
191 markedly distinct temperature tolerance ranges as well as the 10°C difference in optimal growth  
192 temperature between tropical (RS9907 and M16.1) and subpolar strains (MVIR-16-2 and MVIR-18-1),  
193 clearly indicate that these strains correspond to distinct thermotypes (Pittera *et al.*, 2014).

194 All strains were submitted to a stepwise temperature increase and their *in vivo* fluorescence  
195 emission spectra were recorded at each step. During the light-harvesting process, the distal PBP discs  
196 transfer the light excitation energy to the proximal ones, which in turn transfer it to the PBS core. A  
197 low efficiency of energy transfer between two PBPs directly results in an increase in the fluorescence  
198 emitted by the donor PBP, at a specific wavelength. Thus, *in vivo* fluorescence emission spectra  
199 reflect the energy transfer efficiency along the PBS rod down to the reaction center II, and therefore  
200 the overall coupling of the PBS components. As expected from a number of previous studies (Bailey

201 & Grossman, 2008; Six *et al.*, 2004; Six *et al.*, 2005; Six *et al.*, 2007b), the fluorescence emission  
202 spectra typically exhibited three maxima, attributable to PE (565-575 nm), PC (650 nm) and the  
203 combined signal from APC and RC chlorophylls, altogether called the PBS terminal acceptor (TA; 680  
204 nm; Fig. 2A, B). We used the PE:PC emission fluorescence ratio as a parameter integrating the  
205 variations of the fluorescence emitted by the rod PBPs. This therefore allowed us to indirectly  
206 monitor the excitation energy transfer within the PBS rods (Ke, 2001; Six *et al.*, 2007a).

207 PBS performance was strongly affected by the temperature increase and the progressive  
208 alteration followed the same succession of steps in all *Synechococcus* temperature ecotypes. The first  
209 temperature increments (from 22 to 28-31°C, depending on strains) induced no significant change in  
210 the PE:PC emission ratio, showing that the energy was still efficiently transferred along the rod (Fig.  
211 2). As temperature kept increasing, fluorescence first increased in the red region (650-680 nm),  
212 leading to a decrease of the PE:PC ratio (Fig. 2A, B, C). To identify which component between PC and  
213 TA first underwent this energy leak, we carried out a spectral decomposition of the fluorescence  
214 emission spectra (Fig. 2D). Results showed that the first alterations occurred at the TA level (680 nm)  
215 and this energy leak likely mostly originated from chlorophylls bound to the reaction center II,  
216 consistently with a previous report that showed that heat induces a strong chl *a* fluorescence  
217 increase in *Synechocystis* sp. PCC 6803 (Inoue *et al.*, 2001). The reaction center II is indeed known to  
218 be highly sensitive to increases in temperature, which notably causes the oxygen evolving complex to  
219 lose two out of the four Mn atoms of the  $Mn_4CaO_5$  cluster, a dissociation resulting in the breakdown  
220 of oxygen evolution (Kimura *et al.*, 2002).

221 Spectral decompositions further showed that the PC fluorescence component (650 nm) also  
222 increased but at a higher temperature than the reaction center one (Fig. 2D), leading the PE:PC ratio  
223 to keep on decreasing as temperature increased (Fig 2C). This indicates that the reaction center heat-  
224 induced disturbance then propagated to the base of the PBS rod, likely through APC. This energetic  
225 jamming between the reaction center and the base of the PBS, which at this stage was still reversible,  
226 eventually destabilized the whole complex and ultimately led to the dismantling of the PBS. The

227 latter process occurred abruptly and was recognizable by the sudden and large increase in  
228 fluorescence at ~570 nm that indicated the release of free, highly fluorescing PEs in the cytosol (Fig.  
229 2A-B). At this stage, the PBS was irreversibly broken down and light harvesting was no longer  
230 possible. This PBS dismantling phenomenon has been characterized in detail at the transcriptomic,  
231 proteomic, and biophysical levels in several previous studies (Lao & Glazer, 1996; Pittera *et al.*, 2014;  
232 Sah *et al.*, 1998; Six *et al.*, 2007a).

233 By applying an Arrhenius-type analysis (Fig. S1), it was possible to determine accurately the  
234 temperature at which the PBS dismantling occurred,  $T_{\text{PBS}}$ , which we used as an indicator of the  
235 functional PBS thermostability in *in vivo* conditions. This parameter may thus provide information on  
236 the thermal plasticity of the light harvesting function among strains. The comparison of the six strains  
237 grown at different temperatures showed that, in most cases,  $T_{\text{PBS}}$  increased with acclimation  
238 temperature until reaching a plateau (Fig. 3). The apparent enhanced stability of PBS observed for  
239 strains grown at high temperature is most likely due to an increase in the thermotolerance of the  
240 reaction center itself, from where the disturbance originates (Inoue *et al.*, 2001; Nishiyama *et al.*,  
241 2006). Temperature-induced variations of reaction center thermostability are thought to result from  
242 the capability of PsbU and PsbV proteins to stabilize the oxygen evolving complex (Nishiyama *et al.*,  
243 1997; Yamasaki *et al.*, 2002) and/or from adjustments of the fluidity of thylakoid membranes where  
244 the PS II is embedded (Inoue *et al.*, 2001; Loll *et al.*, 2007). The reaction center thermoacclimation  
245 could also be modulated by changes in the D1 protein isoform from D1.1 to the more stable D1.2  
246 (Kós *et al.*, 2008). The difference in the amplitude of the increase of  $T_{\text{PBS}}$  in strains M16.1 and  
247 ROS8604 (Fig. 3A & D) could thus originate in a different PS II composition or in different capacities to  
248 induce such processes.

249 The plateau reached by the  $T_{\text{PBS}}$  parameter was variable and appeared to be related to their  
250 thermal niche of the marine *Synechococcus* strains (Fig. 3). Indeed, strains isolated from subtropical  
251 (M16.1 and RS9907) or warm temperate waters (WH7803) displayed  $T_{\text{PBS}}$  values ranging from 35°C to  
252 43°C whereas the clade I strains isolated from cold temperate and subpolar waters showed

253 significantly lower values between 29°C and 39°C (Wilcoxon test,  $W = 81$ ,  $p\text{-value} < 0.01$ ). These  
254 results show that the PBSs of high latitude strains are functionally less thermostable than the PBSs of  
255 low latitude ones, and therefore suggest that these light-harvesting complexes exhibit different  
256 levels of molecular flexibility. The different thermotypes of marine *Synechococcus* thus use PBSs that  
257 are functionally constrained by temperature.

258

259 ***Differences in phycobilisome molecular flexibility among strains can be explained by differences in***  
260 ***molecular flexibility of individual phycobiliproteins***

261 In the six marine *Synechococcus* strains studied here, PBS rods are made of three classes of  
262 hexameric PBPs, namely PC, PE-I and PE-II, which bind different sets of chromophores and are  
263 maintained together thanks to specific linker polypeptides (Ong & Glazer, 1991; Six *et al.*, 2005; Six *et*  
264 *al.*, 2007b). To understand whether the differences in PBS thermostability among strains are related  
265 to differences in the thermostability of individual PBPs, we first purified all rod PBPs in their native  
266 state, devoid of linker polypeptides. The six strains possess PBPs with identical optical properties,  
267 typical of *Synechococcus* pigment type 3a (Six *et al.*, 2007b), i.e. a PC binding two PEB and one PCB  
268 molecule (so-called R-PC-II; Ong & Glazer, 1987), a PE-I bearing only PEB, and a PE-II binding one PUB  
269 and five PEB molecules (Fig. S2; Ong & Glazer, 1991). The PC, PE-I and PE-II, displayed fluorescence  
270 emission maxima at 635, 569 and 562 nm, respectively. We then performed thermal unfolding curves  
271 for each of these 18 purified PBPs, in order to determine their mid-unfolding temperatures,  $T_{50\%}$ , a  
272 commonly used proxy for assessing and comparing the thermostability and molecular flexibility of  
273 proteins (Fig. S2 & S3; Grimsley *et al.*, 2013; Jaenicke, 1991).

274 Upon temperature increase, all PBPs underwent a progressive drop of absorbance following a  
275 sigmoid curve (Fig. S3), down to levels lower than 10% of the initial value, and at 85°C proteins were  
276 completely unfolded and denatured. Fluorescence also decreased until complete quenching,  
277 following a quasi-linear function (Fig. S4). The comparative analysis of mid-unfolding temperatures  
278 for the three rod PBP types revealed two remarkable trends (Fig. 4). Firstly, the different classes of

279 PBPs showed significantly distinct thermostability (Kruskal-Wallis,  $X^2 = 37.11$ ,  $df = 2$ ,  $p\text{-value} < 0.01$ ).  
280 Indeed, on average, PEII lost half of its absorption capacity at  $60.9 \pm 2.6^\circ\text{C}$ , whereas the mean mid-  
281 unfolding temperature was  $56.0 \pm 2.5^\circ\text{C}$  and  $51.8 \pm 2.0^\circ\text{C}$  for PE-I and PC, respectively. These results  
282 indicate that PBP thermostability decreases towards the core of the PBS rod, with the most distal PE-  
283 II being the most stable PBP and PC the least. The latter finding is quite consistent with our  
284 observation that when cells undergo a moderate temperature shock, PC is the first rod PBP to show  
285 energetic disturbance in the PBS (Fig. 2). As concerns PEII, it is known to be released in the cytosol  
286 under excess light, UV or temperature stress conditions (Pittera *et al.*, 2014; Six *et al.*, 2004; Six *et al.*,  
287 2007a), during which it may constitute a soluble screen dissipating excess excitation energy as  
288 fluorescence, a role that likely requires molecular stability. Secondly, subtropical strains use PBPs  
289 that are significantly more thermostable than strains isolated from cold waters (Fig. 4). While the  
290 southernmost strain M16.1 and RS9907 displayed PEII, PEI and PC  $T_{50\%}$  of  $63.3 \pm 1.2^\circ\text{C}$ ,  $58.4 \pm 0.7^\circ\text{C}$   
291 and  $54.0 \pm 1.0^\circ\text{C}$ , respectively, this parameter was  $5^\circ\text{C}$  lower for the northernmost strains MVIR-16-2  
292 and MVIR-18-1, with corresponding values of  $57.8 \pm 0.4^\circ\text{C}$ ,  $53.4 \pm 1.5^\circ\text{C}$  and  $49.6 \pm 0.4^\circ\text{C}$  (Student t-  
293 test:  $t = 9.68$ ,  $7.49$  and  $10.15$  for PC, PE-I and PE-II, respectively; all  $p\text{-values} < 0.01$ ). Consistently,  
294 mid-unfolding temperatures were strongly correlated to the latitude of strain isolation sites (Fig. S5).  
295 This indicates that the observed differences in overall PBS functional stability among strains isolated  
296 from distinct thermal niches rely at least in part on the differential thermostability of their  
297 constituting PBPs. The distinct thermal unfolding properties of PBPs strongly suggest that the  
298 molecular flexibility of these proteins differs. It is worth noting that the latter experiments were  
299 carried out on PBPs devoid of linker polypeptides, a lack that may somewhat modulate the  
300 thermotolerance of these molecules. Yet, the mid-unfolding temperature values reported here are  
301 quite in the range of previously reported values for other PBPs (Chaiklahan *et al.*, 2012; Edwards *et*  
302 *al.*, 1997; Patel *et al.*, 2004; Pumas *et al.*, 2011; Pumas *et al.*, 2012).

303 To our knowledge, the high latitude *Synechococcus* ecotypes studied here possess the least  
304 thermostable rod PBPs described so far. Indeed, most previous studies have focused on PBPs

305 extracted from thermophilic organisms isolated from hot springs, an environment in which these  
306 complexes require a particularly high thermostability (Adir *et al.*, 2001; Edwards *et al.*, 1997; Munier  
307 *et al.*, 2014). Our study therefore shows that the diversification of PBP variants among PBP-  
308 containing organisms has occurred not only in specific extreme thermal niches, such as hot springs,  
309 but also along the large latitudinal temperature gradients of the Earth.

310

311 ***Marine Synechococcus phycocyanins exhibit molecular characteristics specific of the thermotypes.***

312 In order to unveil possible differences in the molecular conformation of PBs resulting from  
313 adaption to the low temperature niche, as described for other proteins (Croce & van Amerongen,  
314 2014; Závodszy *et al.*, 1998), we analyzed 62 PBP subunit sequences from 21 *Synechococcus* strains  
315 belonging to clades adapted either to cold (I and IV) or warm environments (II and III; Table S1).  
316 Amino acid sequence identity was higher than 80% among MpeA, MpeB, CpeA, RpcA and RpcB, and  
317 70% among CpeB. Analyses of the PBP  $\alpha$ - and  $\beta$ -subunits sequences showed that they exhibit a  
318 number of conserved characteristics. First, the aliphatic index of PBP  $\alpha$ -subunits (RpcA, CpeA and  
319 MpeA) is always lower than that of their  $\beta$ -subunit counterparts (Table 2). This proxy for the relative  
320 volume occupied by aliphatic side chains was shown to be significantly higher in thermostable  
321 proteins (Jollivet *et al.*, 2012; Závodszy *et al.*, 1998). The grand average hydropathy index (GRAVY) is  
322 also different between the two PBP subunits, with  $\alpha$ - being less hydrophobic than  $\beta$ -subunits (Table  
323 2). Consistently,  $\alpha$ -subunits always contain a lower percentage of hydrophobic amino acids than their  
324  $\beta$  counterparts. Thus, even though  $\alpha$ -subunits exhibit a higher content of charged residues than  $\beta$ -  
325 subunits (Dill, 1990; Ladbury *et al.*, 1995),  $\alpha$ -subunits globally appear as the least stable of the two  
326 subunits and the most vulnerable to unfolding factors, such as high temperature, and it thus may  
327 constitute a fragility point within PBP aggregates.

328 Protein molecular adaptations to temperature are known to be in part based on specific  
329 substitutions of amino acids, with glycine, serine, lysine and asparagine in mesophiles, generally  
330 replaced in thermophiles by alanine, threonine, arginine and glutamate, respectively (Argos *et al.*,

331 1979; Fields, 2001; Szilagyi & Zavodszky, 2000). Extensive comparisons of the amino acid content of  
332 each PBP polypeptide revealed that RpcA sequences from members of the warm-environment clade  
333 II had a significantly higher content in alanine than their counterparts from cold clade I strains, *i.e.*  
334  $16.73 \pm 0.36 \%$  and  $15.06 \pm 0.55 \%$ , respectively (Kruskal-Wallis,  $X^2 = 9.83, df = 3, p\text{-value} < 0.05$ ). This  
335 suggests that the observed differential PC thermal unfolding properties between the high and low  
336 latitude strains might partly arise from differences in alanine content. Indeed, alanine accumulation  
337 in proteins is thought to increase hydrophobicity and therefore to decrease molecular flexibility,  
338 notably because this amino acid is an excellent helix former (see *e.g.* Dalhus *et al.*, 2002; Kumwenda  
339 *et al.*, 2013).

340 In contrast to PC, comparative analyses of PE sequences (CpeA, CpeB, MpeA and MpeB) did not  
341 point out any clear evidence of differential amino acid composition that could be related to the  
342 differential thermostability of PEs from subtropical and subpolar strains, possibly due to the fact that  
343 PE genes have been subjected to recurrent lateral transfers during *Synechococcus* evolution  
344 (Everroad & Wood, 2012; Humily *et al.*, 2014; Six *et al.*, 2007b).

345 In order to further understand the possible conformational differences among PCs from different  
346 *Synechococcus* thermotypes, we compared structural homology models of these proteins. Despite a  
347 high overall conservation of the 3D structure of PCs among strains (root mean square deviation <  
348 0.5), we identified two semi-conservative substitutions that are specific of the cold-environment  
349 clades I and IV (Fig. S6). Both of them are located on an exposed domain of helix A (amino acids 35 –  
350 45), which ensures the contact between  $\alpha$  and  $\beta$  subunits (Adir *et al.*, 2006). The first substitution,  
351 located on the  $\alpha$ -43 residue, involves the permutation of alanine found in clades II, III and V to  
352 glycine in clades I and IV. Such a substitution was previously observed when comparing orthologous  
353 proteins of thermophilic vs. mesophilic organisms (Szilagyi & Zavodszky, 2000). Indeed, glycine is  
354 thought to provide increased backbone conformational flexibility (Matthews *et al.*, 1987). The  
355 prediction of protein flexibility allowed us to detect a clear difference in this specific region of the  
356 RpcA chains between cold and warm-environment strains (Fig. 5).

357 Furthermore, the decrease in stability resulting from the substitution from alanine to glycine is  
358 thought to be stronger when it takes place within a helix (Menéndez-Arias & Argosf, 1989; Serrano *et*  
359 *al.*, 1992). Alanine indeed consistently stabilizes helical conformations relatively to glycine, because it  
360 buries more polar areas upon folding and because its backbone entropy is lower. This substitution in  
361 RpcA might thus contribute to the lower stability of PC in the cold-environment *Synechococcus* clades  
362 I and IV compared to warm-environment clades II and III.

363 The second substitution is located on the  $\beta$ -42 residue and involves the replacement of a  
364 serine in cold-environment clades by an asparagine in warm-environment clades (Fig. 6). As this  
365 residue is located on helix A, it likely also participates to the stability of the aggregation between the  
366 PC  $\alpha$ - and  $\beta$ -subunits in the whole  $\alpha\beta$  hexameric aggregate. Furthermore, the structural modeling  
367 showed that this residue is located in the close vicinity of the D cycle of the PEB chromophore bound  
368 to the cysteinyl residue  $\beta$ -152. It is likely that the side chain difference between the asparagine in  
369 cold clades and the serine in warm ones influences the molecular stability of the planar conformation  
370 of the chromophore and therefore its absorption properties. In particular, this substitution is  
371 expected to decrease the steric hindrance and might lead to an increase in flexibility of the  
372 polypeptide chain. It is also important to note that, in such complex protein assemblages, the two  
373 abovementioned substitutions are repeated six times each, resulting in a summation effect that may  
374 greatly impact the overall protein properties.

375

## 376 **Conclusion**

377 Comparative analyses of the photosynthetic antenna complexes of six different marine  
378 *Synechococcus* strains isolated from different latitudes revealed clade-specific adaptations to  
379 temperature that are likely critical to maintain the biophysical properties of these pigment-protein  
380 complexes in the specific thermal niches of these strains. This result nicely complements previous  
381 work (Pittera *et al.*, 2014), which showed that the sensitivity of the light-harvesting process to  
382 temperature variations was thermotype-dependent and that the thermo-resistance of PBS

383 complexes was directly associated with the growth capacities of the considered strain. Altogether,  
384 these complementary studies suggest that the thermoadaptability of light-harvesting complexes  
385 likely plays a key role in the wide latitudinal distribution of thermotypes (Farrant *et al.*, 2016; Sohm  
386 *et al.*, 2015), although other factors are certainly also involved, such as different membrane  
387 composition adjustments or of heat shock proteins and/or antifreeze metabolites.

388 The functional differences between PBSs of cold- and warm-environment strains are seemingly  
389 due to large differences in the molecular flexibility of the three PBPs constituting the rods. *In vivo*  
390 temperature response curves indicated that PC is the first rod PBP to undergo energetic decoupling,  
391 which then propagates through the entire rod, until complete dismantling of the PBS complex.  
392 Consistently, we show that among the three rod PBPs, PC is the least thermostable and probably  
393 constitutes a fragility point of the PBS rod under heat stress. Our results suggest that the  
394 thermotype-specific differences in the stability or flexibility of PC originate at least in part from the  
395 modulation of the alanine content as well as from two amino acid substitutions. We hypothesize that  
396 temperature has exerted significant adaptive pressure on PBP evolution in marine *Synechococcus*,  
397 conferring a fitness advantage to cold-adapted strains at high latitude, as shown by their specific  
398 ability to grow and photosynthesize at low temperature (Pittera *et al.*, 2014). Further evidence for  
399 the central role of the trade-off between PBP flexibility and stability for adaptation to cold and warm  
400 niches, respectively, could be obtained from directed mutagenesis targeting the amino acids that we  
401 found to differ between the PCs of cold and warm thermotypes. Yet, such genetic manipulation  
402 remains a challenging task in marine picocyanobacteria.

403 In many organisms, including marine picocyanobacteria (Johnson *et al.*, 2006; Moore *et al.*, 1995;  
404 Pittera *et al.*, 2014), maximal growth-rate temperature occurs very close to the cell death  
405 temperature and physiological models suggest that the latter temperature coincides with a  
406 denaturation catastrophe of the proteome (Dill *et al.*, 2011). The high sensitivity of protein structure  
407 and function to temperature variations indicates that the ongoing global climate change is likely to  
408 affect cells through perturbation of enzymatic and structural proteins. The evolutionary process

409 described here, which is a component of the thermotypic diversification occurring in several major  
410 *Synechococcus* lineages, is probably one of the key factors explaining the global ecological success of  
411 these cyanobacteria. Elucidating such processes is important in the context of global climate change  
412 as the latter will undoubtedly induce alterations of the composition of the phytoplanktonic  
413 communities over large oceanic spatial scales and thus impact top levels of food webs.

414

415       Supplementary information is available at ISMEJ's website.

416

## 417 **Acknowledgments**

418       This work was funded by the French program ANR SAMOSA (ANR-13-ADAP-0010), EMBRC France  
419 (INFRA-2010-2.2.5) and the European Union programs MicroB3 and MaCuMBA (grant agreements  
420 287589 and 311975, respectively). Justine Pittera was supported by the French Ministry of Higher  
421 Education and Research. We warmly thank Laurence Garczarek, Florian Humily and Morgane Ratin  
422 for providing us new phycobiliprotein sequences retrieved from unpublished genomes sequenced by  
423 the Genoscope (Evry, France) and assembled with the help of Gregory Farrant and the local  
424 bioinformatics platform (ABIMS, Roscoff, France). We are also grateful to the Roscoff Culture  
425 Collection for maintaining the *Synechococcus* strains used in this study and especially to Florence  
426 Legall who isolated some of them. We certify that there is no conflict of interest with any financial  
427 organization regarding the material presented in this manuscript.

428

429 **References**

430 Adir N, Dobrovetsky Y & Lerner N (2001). Structure of C-phycoyanin from the thermophilic  
431 cyanobacterium *Synechococcus vulcanus* at 2.5 Å: structural implications for thermal stability  
432 in phycobilisome assembly. *J Mol Biol* **313**: 71-81.

433

434 Adir N, Dines M, Klartag M, McGregor A & Melamed-Frank M (2006). Assembly and  
435 disassembly of phycobilisomes. In: Shively J (ed). *Complex intracellular structures in*  
436 *prokaryotes*. Springer-Verlag: Berlin Heidelberg, Germany. pp 47-77.

437

438 Ahlgren N & Rocap G (2012). Diversity and distribution of marine *Synechococcus*: Multiple  
439 gene phylogenies for consensus classification and development of qPCR assays for sensitive  
440 measurement of clades in the ocean. *Front Microbiol* **3**: doi: 10.3389/fmicb.2012.00213.

441

442 Argos P, Rossmann M, Grau U, Zuber H, Frank G & Tratschin J (1979). Thermal stability and  
443 protein structure. *Biochemistry* **18**: 5698-5703.

444

445 Bailey S & Grossman A (2008). Photoprotection in cyanobacteria: Regulation of light  
446 harvesting. *Photochem Photobiol* **84**: 1410-1420.

447

448 Behrenfeld M, O'Malley R, Siegel D, McClain C, Sarmiento J, Feldman G *et al.* (2006). Climate-  
449 driven trends in contemporary ocean productivity. *Nature* **444**: 752-755.

450

451 Berman H, Henrick K & Nakamura H (2003). Announcing the worldwide Protein Data Bank.  
452 *Nat Struct Mol Biol* **10**: 980.

453

454 Blot N, Wu X, Thomas J-C, Zhang J, Garczarek L, Böhm S *et al.* (2009). Phycourobilin in  
455 trichromatic phycocyanin from oceanic cyanobacteria is formed post-translationally by a  
456 phycoerythrobilin lyase-isomerase. *J Biol Chem* **284**: 9290-9298.

457

458 Bowen R, Hartung R & Gindt Y (2000). A simple protein purification and folding experiment  
459 for general chemistry laboratory. *J Chem Educ* **77**: 1456.

460

461 Chaiklahan R, Chirasuwan N & Bunnag B (2012). Stability of phycocyanin extracted from  
462 *Spirulina* sp.: influence of temperature, pH and preservatives. *Process Biochem* **47**: 659-664.

463

464 Croce R & van Amerongen H (2014). Natural strategies for photosynthetic light harvesting.  
465 *Nat Chem Biol* **10**: 492-501.

466

467 Dahlhoff E, O'Brien J, Somero G & Vetter R (1991). Temperature effects on mitochondria  
468 from hydrothermal vent invertebrates: Evidence for adaptation to elevated and variable  
469 habitat temperatures. *Physiol Zool* **64**: 1490-1508.

470

471 Dalhus B, Saarinen M, Sauer U, Eklund P, Johansson K, Karlsson A *et al.* (2002). Structural  
472 basis for thermophilic protein stability: Structures of thermophilic and mesophilic malate  
473 dehydrogenases. *J Mol Biol* **318**: 707-721.

474

475 Dill K (1990). Dominant forces in protein folding. *Biochemistry* **29**: 7133-7155.

476

477 Dill K, Ghosh K & Schmit J (2011). Physical limits of cells and proteomes. *Proc Natl Acad Sci*  
478 *USA* **108**: 17876-17882.

479

480 Edwards M, Hauer C, Stack R, Eisele L & MacColl R (1997). Thermophilic C-phycoyanin:  
481 effect of temperature, monomer stability, and structure. *Biochim Biophys Acta* **1321**: 157-  
482 164.

483

484 Everroad R & Wood A (2012). Phycoerythrin evolution and diversification of spectral  
485 phenotype in marine *Synechococcus* and related picocyanobacteria. *Mol Phylogen Evol* **64**:  
486 381-392.

487

488 Falkowski P (1994). The role of phytoplankton photosynthesis in global biochemical cycles.  
489 *Photosynth Res* **39**: 235-258.

490

491 Farrant G, Doré D, Cornejo-Castillo F, Partensky F, Ratin M, Ostrowski M *et al.* (2016).  
492 Delineating ecologically significant taxonomic units from global patterns of marine  
493 picocyanobacteria. *Proc Nat Acad Sci USA* **in revision**.

494

495 Fields P (2001). Review: Protein function at thermal extremes: balancing stability and  
496 flexibility. *Comp Biochem Physiol Pt A* **129**: 417-431.

497

498 Flombaum P, Gallegos J, Gordillo R, Rincón J, Zabala L, Jiao N *et al.* (2013). Present and future  
499 global distributions of the marine cyanobacteria *Prochlorococcus* and *Synechococcus*. *Proc*  
500 *Natl Acad Sci USA* **110**: 9824-9829.

501

502 Fuller NJ, Marie D, Partensky F, Vaulot D, Post A & Scanlan D (2003). Clade-specific 16S  
503 ribosomal DNA oligonucleotides reveal the predominance of a single marine *Synechococcus*  
504 clade throughout a stratified water column in the Red Sea. *Appl Environ Microbiol* **69**: 2430-  
505 2443.

506

507 Gasteiger E, Hoogland C, Gattiker A, Duvaud S, Wilkins M, Appel R *et al.* (2005). Protein  
508 identification and analysis tools on the ExPASy Server. In: Walker J (ed). *The Proteomics*  
509 *Protocols Handbook*. Humana Press: Totowa, NJ. pp 571-607.

510

511 Glazer A, Fang S & Brown D (1973). Spectroscopic properties of C-phycoyanin and of its  $\alpha$   
512 and  $\beta$  subunits. *J Biol Chem* **248**: 5679-5685.

513

514 Glazer A & Hixson C (1975). Characterization of R-phycoyanin. Chromophore content of R-  
515 phycoyanin and C-phycoerythrin. *J Biol Chem* **250**: 5487-5495.

516

517 Glazer A & Hixson C (1977). Subunit structure and chromophore composition of  
518 rhodophytan phycoerythrins. *Porphyridium cruentum* B-phycoerythrin and b-phycoerythrin.  
519 *J Biol Chem* **252**: 32-42.

520

521 Glazer A (1984). Phycobilisome a macromolecular complex optimized for light energy  
522 transfer. *Biochim Biophys Acta* **768**: 29-51.

523

524 Glazer A (1985). Light harvesting by phycobilisomes. *Ann Rev Biophys Biophys Chem* **14**: 47-  
525 77.

526

527 Glazer A (1989). Light guides. Directional energy transfer in a photosynthetic antenna. *J Biol*  
528 *Chem* **264**: 1-4.

529

530 Grimsley G, Trevino S, Thurlkill R & Scholtz J (2013). Determining the conformational stability  
531 of a protein from urea and thermal unfolding curves. *Curr Prot Protein Sci* **28**: doi:  
532 10.1002/0471140864.

533

534 Hall TA (1999). BioEdit: a user-friendly biological sequence alignment editor and analysis  
535 program for Windows 95/98/NT. *Nucleic Acids Symp Ser* **41**: 95-98.

536

537 Herdman M, Castenholz R, Waterbury J & Rippka R (2001). Form-genus XIII. *Synechococcus*.  
538 In: Boone D, Castenholz R (eds). *Bergey's Manual of Systematic Bacteriology*, 2d Ed. edn.  
539 Springer-Verlag: New York. pp 508-512.

540

541 Huang S, Wilhelm S, Harvey H, Taylor K, Jiao N & Chen F (2012). Novel lineages of  
542 *Prochlorococcus* and *Synechococcus* in the global oceans. *ISME J* **6**: 285-297.

543

544 Humily F, Partensky F, Six C, Farrant G, Ratin M, Marie D *et al.* (2013). A gene island with two  
545 possible configurations is involved in chromatic acclimation in marine *Synechococcus*. *PLoS*  
546 *ONE* **8**: e84459.

547

548 Humily F, Farrant G, Marie D, Partensky F, Mazard S, Perennou M *et al.* (2014). Development  
549 of a targeted metagenomic approach to study a genomic region involved in light harvesting  
550 in marine *Synechococcus*. *FEMS Microbiol Ecol* **88**: 231-249.

551

552 Inoue N, Taira Y, Emi T, Yamane Y, Kashino Y, Koike H *et al.* (2001). Acclimation to the growth  
553 temperature and the high-temperature effects on photosystem II and plasma membranes in  
554 a mesophilic cyanobacterium, *Synechocystis* sp PCC6803. *Plant Cell Physiol* **42**: 1140-1148.

555

556 Jaenicke R (1991). Protein folding: local structures, domains, subunits, and assemblies.  
557 *Biochemistry* **30**: 3147-3161.

558

559 Jaenicke R & Böhm G (1998). The stability of proteins in extreme environments. *Curr Opin*  
560 *Struct Biol* **8**: 738-748.

561

562 Jiang T, Zhang J-P, Chang W-R & Liang D-C (2001). Crystal structure of R-phycoyanin and  
563 possible energy transfer pathways in the phycobilisome. *Biophys J* **81**: 1171-1179.

564

565 Johnson Z, Zinser E, Coe A, McNulty N, Woodward E & Chisholm S (2006). Niche partitioning  
566 among *Prochlorococcus* ecotypes along ocean-scale environmental gradients. *Science* **311**:  
567 1737-1740.

568

569 Jollivet D, Mary J, Gagnière N, Tanguy A, Fontanillas E, Boutet I *et al.* (2012). Proteome  
570 adaptation to high temperatures in the ectothermic hydrothermal vent Pompeii worm. *PLoS*  
571 *One* **7**: e31150.

572

573 Katoh K & Standley D (2013). MAFFT Multiple sequence alignment software version 7:  
574 Improvements in performance and usability. *Mol Biol Evol* **30**: 772-780.

575

576 Ke B (2001). Phycobiliproteins and phycobilisomes. In: Ke B (ed). *Photosynthesis:  
577 Photobiochemistry and photobiophysics*. Kluwer Academic Publishers: Dordrecht. pp 253-  
578 270.

579

580 Kelley L & Sternberg M (2009). Protein structure prediction on the Web: a case study using  
581 the Phyre server. *Nat Protocols* **4**: 363-371.

582

583 Kimura A, Eaton-Rye J, Morita E, Nishiyama Y & Hayashi H (2002). Protection of the oxygen-  
584 evolving machinery by the extrinsic proteins of photosystem II is essential for development  
585 of cellular thermotolerance in *Synechocystis* sp. PCC 6803. *Plant Cell Physiol* **43**: 932-938.

586

587 Kós P, Deák Z, Cheregi O & Vass I (2008). Differential regulation of *psbA* and *psbD* gene  
588 expression, and the role of the different D1 protein copies in the cyanobacterium  
589 *Thermosynechococcus elongatus* BP-1. *Biochim Biophys Acta* **1777**: 74-83.

590

591 Kumwenda B, Litthauer D, Bishop O & Reva O (2013). Analysis of protein thermostability  
592 enhancing factors in industrially important *Thermus* bacteria species. *Evol Bioinfo Online* **9**:  
593 327-342.

594

595 Kupper H, Andresen E, Wiegert S, Simek M, Leitenmaier B & Setlik I (2009). Reversible  
596 coupling of individual phycobiliprotein isoforms during state transitions in the  
597 cyanobacterium *Trichodesmium* analysed by single-cell fluorescence kinetic measurements.  
598 *Biochim Biophys Acta* **1787**: 155-167.

599

600 Ladbury J, Lemmon M, Zhou M, Green J, Botfield M & Schlessinger J (1995). Measurement of  
601 the binding of tyrosyl phosphopeptides to SH2 domains: a reappraisal. *Proc Natl Acad Sci*  
602 *USA* **92**: 3199-3203.

603

604 Lao K & Glazer A (1996). Ultraviolet-B photodestruction of a light-harvesting complex. *Proc*  
605 *Natl Acad Sci USA* **93**: 5258-5263.

606

607 Loll B, Kern J, Saenger W, Zouni A & Biesiadka J (2007). Lipids in photosystem II: Interactions  
608 with protein and cofactors. *Biochim Biophys Acta* **1767**: 509-519.

609

610 MacColl R, Csatorday K, Berns D & Traeger E (1980). Chromophore interactions in  
611 allophycocyanin. *Biochemistry* **19**: 2817-2820.

612

613 Mackey K, Paytan A, Caldeira K, Grossman A, Moran D, McIlvin M *et al.* (2013). Effect of  
614 temperature on photosynthesis and growth in marine *Synechococcus* spp. *Plant Physiol* **163**:  
615 815-829.

616

617 Matthews B, Nicholson H & Becktel W (1987). Enhanced protein thermostability from site-  
618 directed mutations that decrease the entropy of unfolding. *Proc Natl Acad Sci USA* **84**: 6663-  
619 6667.

620

621 Mazard S, Ostrowski M, Partensky F & Scanlan D (2012). Multi-locus sequence analysis,  
622 taxonomic resolution and biogeography of marine *Synechococcus*. *Environ Microbiol* **14**: 372-  
623 386.

624

625 Mella-Flores D, Mazard S, Humily F, Partensky F, Mahé F, Bariat L *et al.* (2011). Is the  
626 distribution of *Prochlorococcus* and *Synechococcus* ecotypes affected by global warming?  
627 *Biogeosciences* **8**: 2785-2804.

628

629 Menéndez-Arias L & Argosf P (1989). Engineering protein thermal stability. *J Mol Biol* **206**:  
630 397-406.

631

632 Moore L, Goericke R & Chisholm S (1995). Comparative physiology of *Synechococcus* and  
633 *Prochlorococcus*: influence of light and temperature on growth, pigments, fluorescence and  
634 absorptive properties. *Mar Ecol Prog Ser* **116**: 259-275.

635

636 Munier M, Jubeau S, Wijaya A, Morançais M, Dumay J, Marchal L *et al.* (2014).  
637 Physicochemical factors affecting the stability of two pigments: R-phycoerythrin of  
638 *Grateloupia turuturu* and B-phycoerythrin of *Porphyridium cruentum*. *Food Chem* **150**: 400-  
639 407.

640

641 Murata N, Takahashi S, Nishiyama Y & Allakhverdiev S (2007). Photoinhibition of  
642 photosystem II under environmental stress. *Biochim Biophys Acta* **1767**: 414-421.

643

644 Neuer S (1992). Growth dynamics of marine *Synechococcus* spp. in the Gulf of Alaska. *Mar*  
645 *Ecol Prog Ser* **83**: 251-262.

646

647 Nishiyama Y, Los D, Hayashi H & Murata N (1997). Thermal Protection of the oxygen-  
648 evolving machinery by PsbU, an extrinsic protein of photosystem II, in *Synechococcus* sp PCC  
649 7002. *Plant Physiol* **115**: 1473-1480.

650

651 Nishiyama Y, Allakhverdiev S & Murata N (2006). A new paradigm for the action of reactive  
652 oxygen species in the photoinhibition of photosystem II. *Biochim Biophys Acta* **1757**: 742-  
653 749.

654

655 Ong L & Glazer A (1987). R-phycoerythrin II, a new phycoerythrin occurring in marine  
656 *Synechococcus* species. Identification of the terminal energy acceptor bilin in phycoerythrins. *J*  
657 *Biol Chem* **262**: 6323-6327.

658

659 Ong L & Glazer A (1991). Phycoerythrins of marine unicellular cyanobacteria. 1. Bilin types  
660 and locations and energy-transfer pathways in *Synechococcus* spp. phycoerythrins. *J Biol*  
661 *Chem* **266**: 9515-9527.

662

663 Padyana A, Bhat V, Madyastha K, Rajashankar K & Ramakumar S (2001). Crystal structure of  
664 a light-harvesting protein C-Phycocyanin from *Spirulina platensis*. *Biochem Biophys Res*  
665 *Commun* **282**: 893-898.

666

667 Partensky F, Blanchot J & Vaulot D (1999). Differential distribution and ecology of  
668 *Prochlorococcus* and *Synechococcus* in oceanic waters: a review. In: Charpy L, Larkum A  
669 (eds). *Marine Cyanobacteria*. Bull Instit Oceanogr Monaco. pp 457-475.

670

671 Patel A, Pawar R, Mishra S, Sonawane S & Ghosh P (2004). Kinetic studies on thermal  
672 denaturation of C-phycoyanin. *Indian J Biochem Biophys* **41**: 254-257.

673

674 Pittera J, Humily F, Thorel M, Grulois D, Garczarek L & Six C (2014). Connecting thermal  
675 physiology and latitudinal niche partitioning in marine *Synechococcus*. *ISME J* **8**: 1221-1236.

676

677 Pumas C, Vacharapiyasophon P, Peerapornpisal Y, Leelapornpisid P, Boonchum W, Ishii M *et*  
678 *al.* (2011). Thermostability of phycobiliproteins and antioxidant activity from four  
679 thermotolerant cyanobacteria. *Phycol Res* **59**: 166-174.

680

681 Pumas C, Peerapornpisal Y, Vacharapiyasophon P, Leelapornpisid P, Boonchum W, Ishii M *et*  
682 *al.* (2012). Purification and characterization of a thermostable phycoerythrin from hot spring  
683 cyanobacterium *Leptolyngbya* sp. KC45. *Int J Agric Biol* **14**: 121-125.

684

685 Rippka R, Coursin T, Hess W, Lichtlé C, Scanlan DJ, Palinska KA *et al.* (2000). *Prochlorococcus*  
686 *marinus* Chisholm *et al.* 1992 subsp. *pastoris* subsp. nov. strain PCC 9511, the first axenic

687 chlorophyll a2/b2-containing cyanobacterium (Oxyphotobacteria). *Intl J Syst Evol Microbiol*  
688 **50**: 1833-1847.

689

690 Sah J, Krishna K, Srivastava M & Mohanty P (1998). Effects of ultraviolet-B radiation on  
691 phycobilisomes of *Synechococcus* PCC 7942: alterations in conformation and energy transfer  
692 characteristics. *IUBMB Life* **44**: 245-257.

693

694 Scheer H & Kufer W (1977). Conformational studies on C-phycocyanin from *Spirulina*  
695 *platensis*. *Z Naturforsch* **32c**: 513-519.

696

697 Serrano L, Sancho J, Hirshberg M & Fersht A (1992).  $\alpha$ -Helix stability in proteins: I. Empirical  
698 correlations concerning substitution of side-chains at the N and C-caps and the replacement  
699 of alanine by glycine or serine at solvent-exposed surfaces. *J Mol Biol* **227**: 544-559.

700

701 Sidler W (1994). Phycobilisome and phycobiliprotein structures. In: Bryant D (ed). *The*  
702 *Molecular Biology of Cyanobacteria*. Kluwer Academic Publishers: Dordrecht, The  
703 Netherlands. pp 139-216.

704

705 Six C, Thomas J-C, Brahamsha B, Lemoine Y & Partensky F (2004). Photophysiology of the  
706 marine cyanobacterium *Synechococcus* sp. WH8102, a new model organism. *Aquat Microb*  
707 *Ecol* **35**: 17-29.

708

709 Six C, Thomas J-C, Thion L, Lemoine Y, Zal F & Partensky F (2005). Two novel phycoerythrin-  
710 associated linker proteins in the marine cyanobacterium *Synechococcus* sp strain WH8102. *J*  
711 *Bacteriol* **187**: 1685-1694.

712

713 Six C, Joubin L, Partensky F, Holtzendorff J & Garczarek L (2007a). UV-induced phycobilisome  
714 dismantling in the marine picocyanobacterium *Synechococcus* sp. WH8102. *Photosynth Res*  
715 **92**: 75-86.

716

717 Six C, Thomas J, Garczarek L, Ostrowski M, Dufresne A, Blot N *et al.* (2007b). Diversity and  
718 evolution of phycobilisomes in marine *Synechococcus* spp. - a comparative genomics study.  
719 *Genome Biol* **8**: R259.

720

721 Sohm J, Ahlgren N, Thomson Z, Williams C, Moffett J, Saito M *et al.* (2015). Co-occurring  
722 *Synechococcus* ecotypes occupy four major oceanic regimes defined by temperature,  
723 macronutrients and iron. *ISME J* **10**: 333-345.

724

725 Stillman J & Somero G (1996). Adaptation to temperature stress and aerial exposure in  
726 congeneric species of intertidal porcelain crabs (genus *Petrolisthes*): correlation of  
727 physiology, biochemistry and morphology with vertical distribution. *J Exp Biol* **199**: 1845-  
728 1855.

729

730 Szilagyi A & Zavodszky P (2000). Structural differences between mesophilic, moderately  
731 thermophilic and extremely thermophilic protein subunits: results of a comprehensive  
732 survey. *Structure* **8**: 493-504.

733

734 Wyman M (1992). An in vivo method for the estimation of phycoerythrin concentrations in  
735 marine cyanobacteria (*Synechococcus* spp.). *Limnol Oceanogr* **37**: 1300-1306.

736

737 Yamasaki T, Yamakawa T, Yamane Y, Koike H, Satoh K & Katoh S (2002). Temperature  
738 acclimation of photosynthesis and related changes in photosystem II electron transport in  
739 winter wheat. *Plant Physiol* **128**: 1087-1097.

740

741 Závodszky P, Kardos J, Svingor Á & Petsko G (1998). Adjustment of conformational flexibility  
742 is a key event in the thermal adaptation of proteins. *Proc Natl Acad Sci USA* **95**: 7406-7411.

743

744 Zinser E, Johnson Z, Coe A, Karaca E, Veneziano D & Chisholm S (2007). Influence of light and  
745 temperature on *Prochlorococcus* ecotype distributions in the Atlantic Ocean. *Limnol*  
746 *Oceanogr* **52**: 2205-2220.

747

748 Zwirgmaier K, Jardillier L, Ostrowski M, Mazard S, Garczarek L, Vaulot D *et al.* (2008). Global  
749 phylogeography of marine *Synechococcus* and *Prochlorococcus* reveals a distinct partitioning  
750 of lineages among oceanic biomes. *Environ Microbiol* **10**: 147-161.

751

752

753

754 **Figure legends**

755 **Figure 1:** Isolation sites of the six marine *Synechococcus* strains used in this study. Squares, diamonds  
756 and circles correspond to subtropical, temperate and subpolar strains, respectively. Colors indicate  
757 the mean average annual sea surface temperature (MODIS) over the 2004-2014 period (QGIS 2.10.1).

758 **Figure 2:** Examples of variations of the fluorescence emission spectra (with excitation at 530 nm) for  
759 the tropical *Synechococcus* strain M16.1 and the subpolar strain MVIR-16-2 acclimated at 22°C and  
760 submitted to a progressive temperature increase. Fluorescence emission spectra of M16.1 **(A)** and  
761 MVIR-16-2 **(B)** strains at different temperatures. **(C)** Variations of the PE:PC (570:650nm)  
762 fluorescence emission ratio during the course of temperature increase in both strains, expressed as  
763 percentage of the initial value (at 22°C). **(D)** Relative variations of fluorescence intensity expressed as  
764 percentage of the initial fluorescence value, after spectral decomposition of the two red  
765 components: phycocyanin at 650 nm (dashed line) and terminal acceptor at 680 nm (solid line). Note  
766 that the APC fluorescence component of the 680 nm peak cannot be easily separated from that of RC  
767 chlorophylls in decomposed spectra but it is expected to be much lower.

768 **Figure 3:** Phycobilisome breaking temperature as a function of growth temperature for the six tested  
769 marine *Synechococcus* strains: M16.1 **(A)**, RS9907 **(B)**, WH7803 **(C)**, ROS8604 **(D)**, MVIR-16-2 **(E)**,  
770 MVIR-18-1 **(F)**. Three replicates are shown. Tropical strains are represented by squares, temperate  
771 ones by diamonds, and subpolar strains by circles.

772 **Figure 4:** Mid-unfolding temperature of the three PBP of the six marine *Synechococcus* strains,  
773 derived from the thermal unfolding curves (see Fig. S2 & S3). Error bars are standard deviation from  
774 the mean based on at least three replicates.

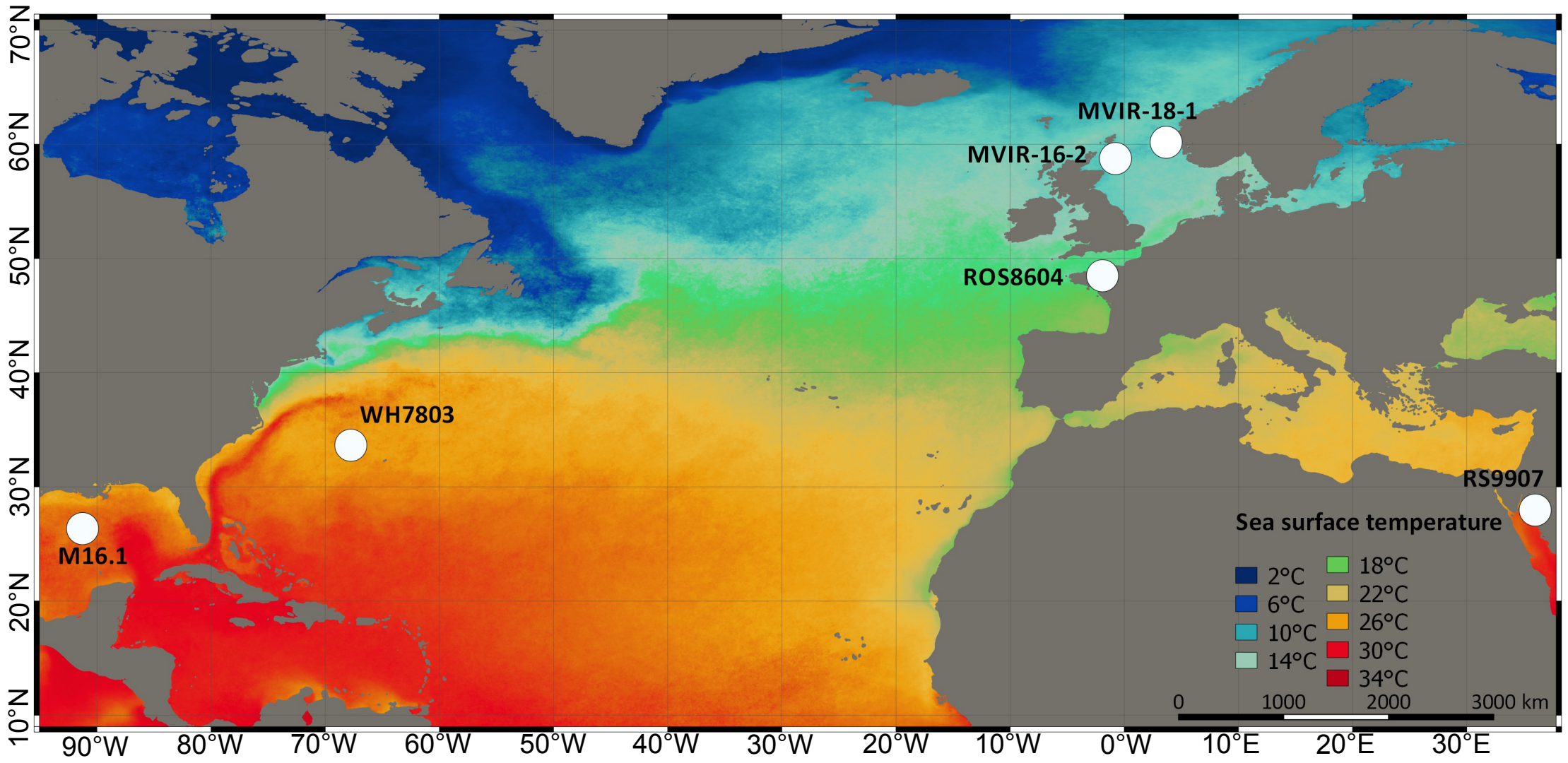
775 **Figure 5:** Predicted average flexibility along the amino acid sequence of phycocyanin  $\alpha$ -subunit  
776 (R<sub>pcA</sub>) for *Synechococcus* strains of the cold-environment clades I and IV (dark blue, light blue,  
777 respectively), and the warm-environment clades II and III (orange and red, respectively). Error bars

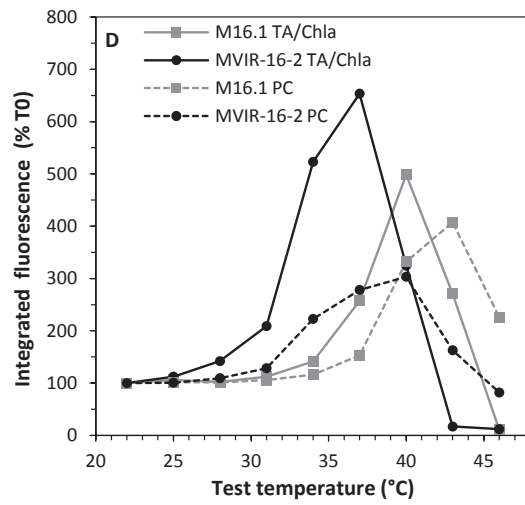
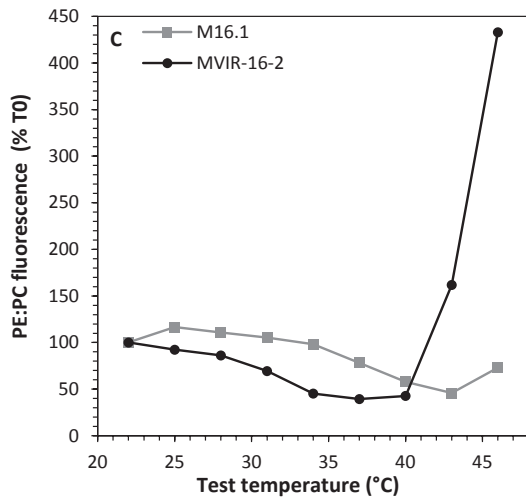
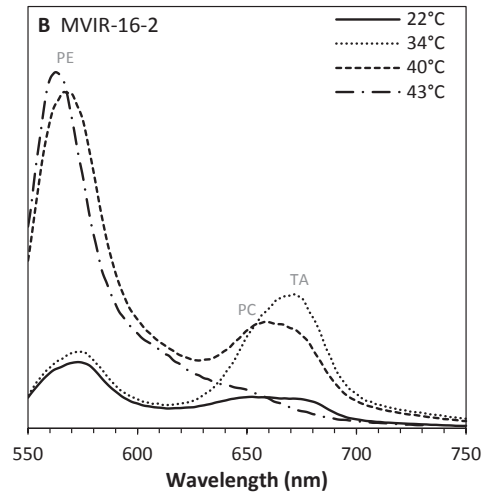
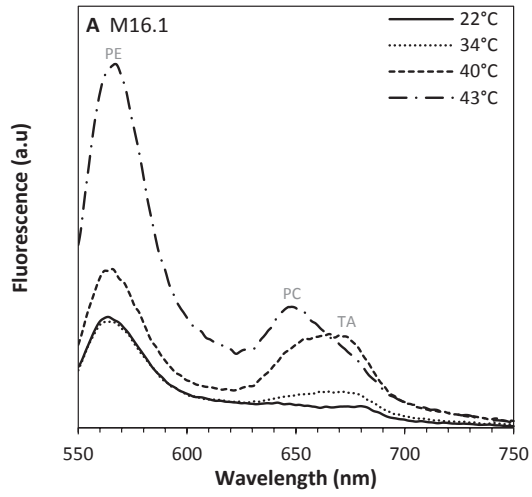
778 are calculated from the mean of 5, 9, 5 and 2 sequences for clades I, II, III and IV, respectively (see  
779 Table S1). The amino acid chain flexibility level was calculated using the ExPasy tool ProtScale  
780 (Gasteiger *et al.*, 2005). The insert shows the only major flexibility difference at the clade specific  
781 substitution.

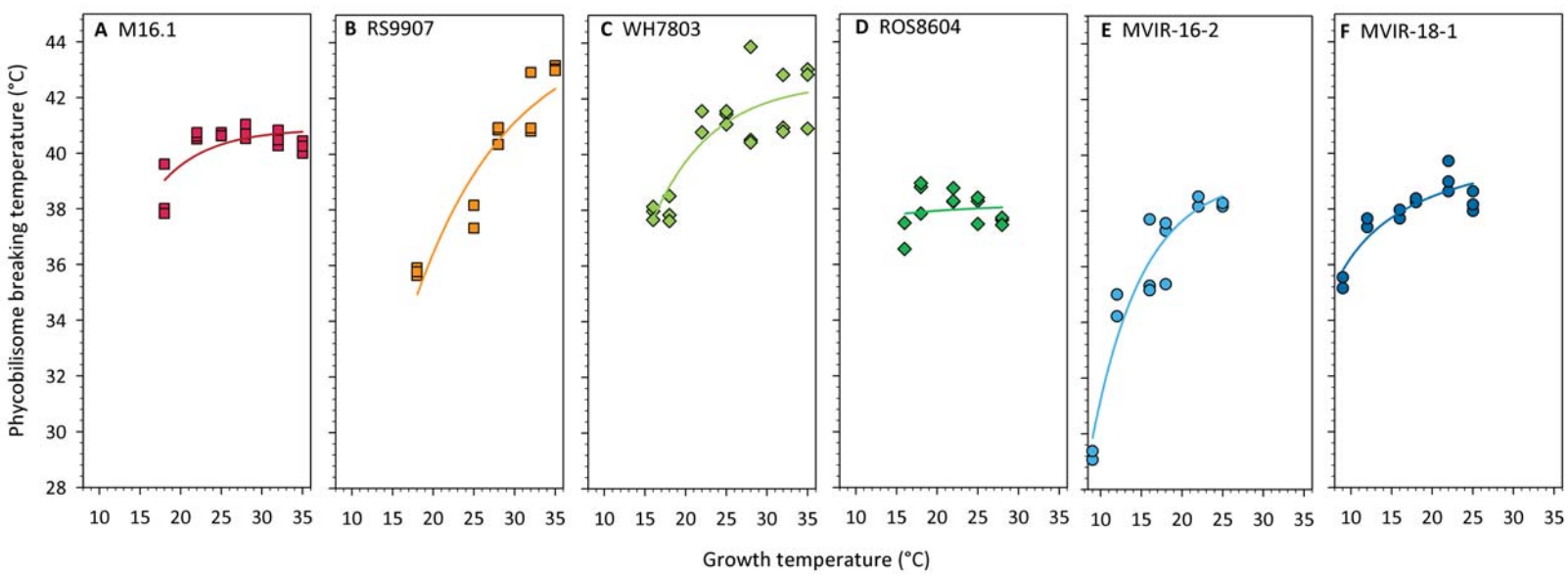
782 **Figure 6:** Computational homology model of an R-phycoerythrin (R-PC-II) trimer structure of the  
783 subpolar strain *Synechococcus* sp. MVIR-18-1 and structural differences with the subtropical strain  
784 M16.1 R-PC-II. **(A)** Upper view of the R-PC-II trimer with  $\alpha$ -subunits (RpcA) in blue and  $\beta$ -subunits  
785 (RpcB) in pink. On each subunit, the amino acid substitutions specific to cold-environment clades,  
786 located at  $\alpha$ -43 and  $\beta$ -42, are shown in red. Phycoerythrobilins (PEB) are shown in dark pink and  
787 phycocyanobilins (PCB) in blue. **(B)** Side view of a PC monomer, showing the location of the  
788 substitution sites on helix A, involved in the  $\alpha$ - $\beta$  subunit interaction in *Synechococcus* sp. MVIR-18-1.  
789 **(C)** Zoom in the  $\beta$ -42 substitution with the subpolar strain *Synechococcus* sp. MVIR-18-1 displaying a  
790 serine and the subtropical *Synechococcus* sp. M16.1 displaying an asparagine **(D)**.

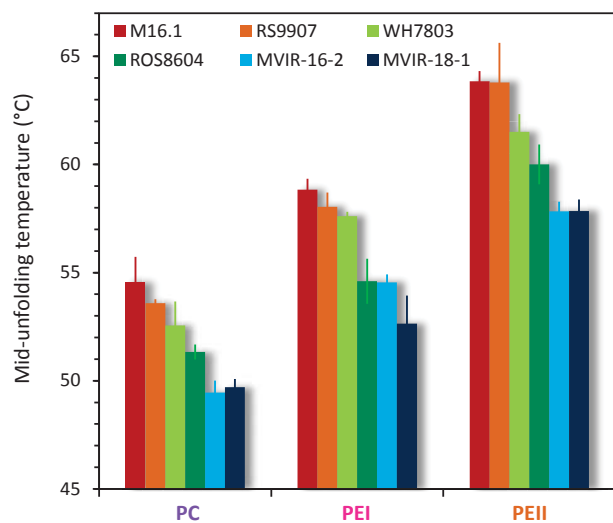
791  
792

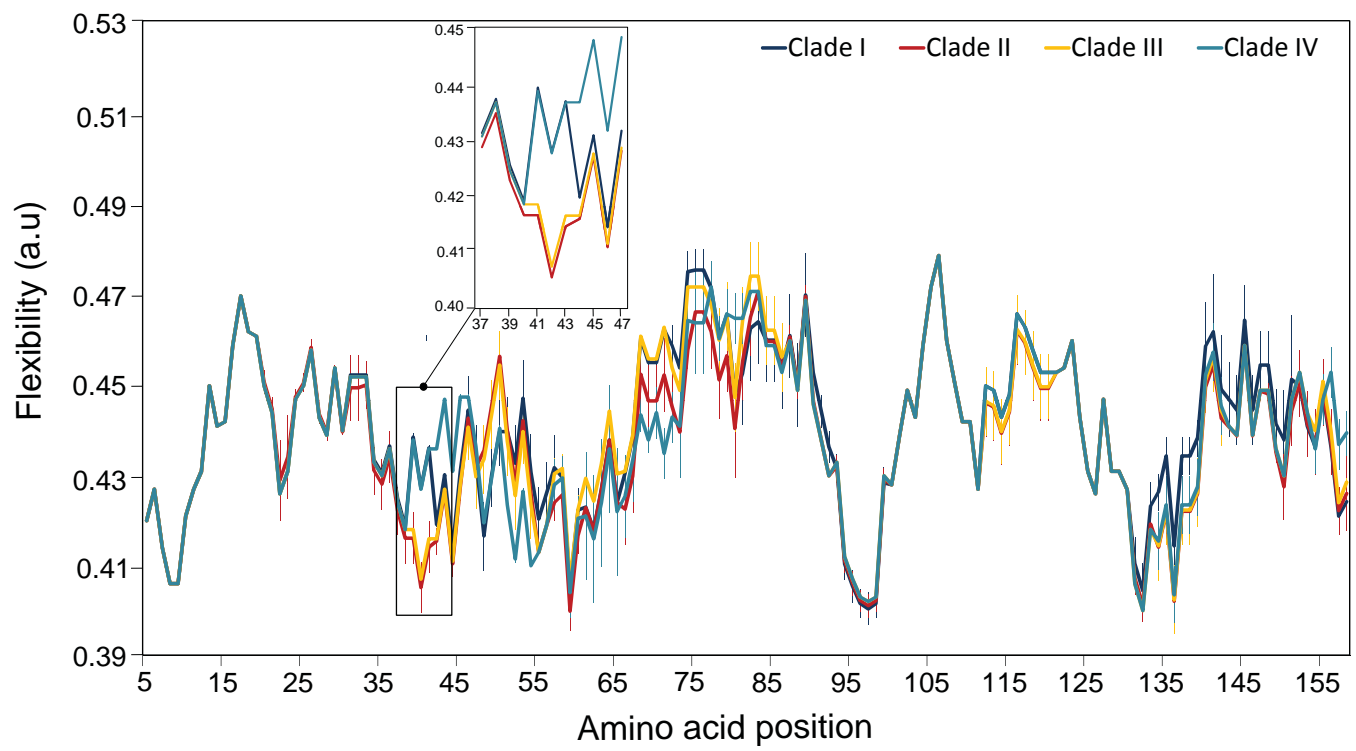
793

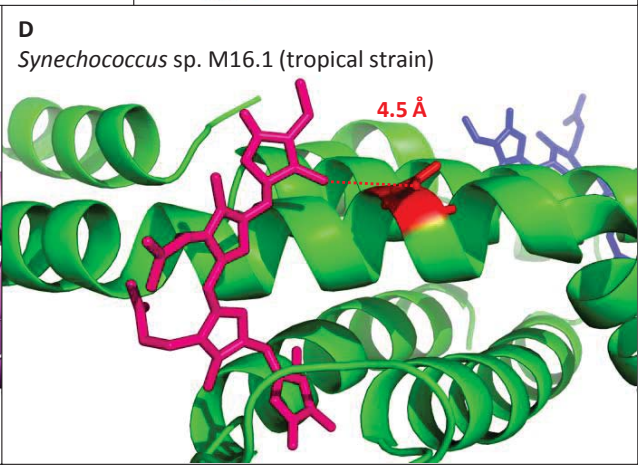
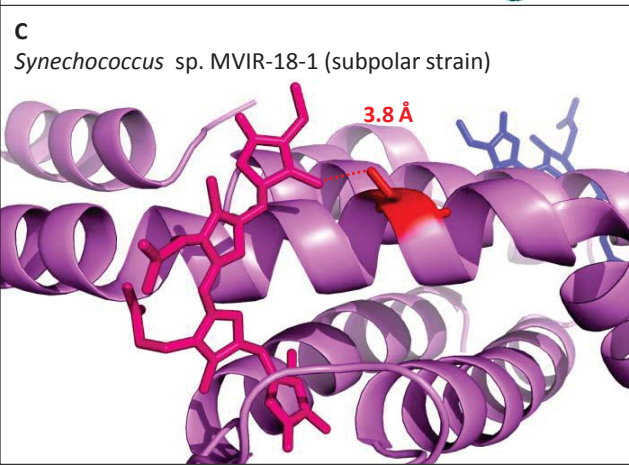
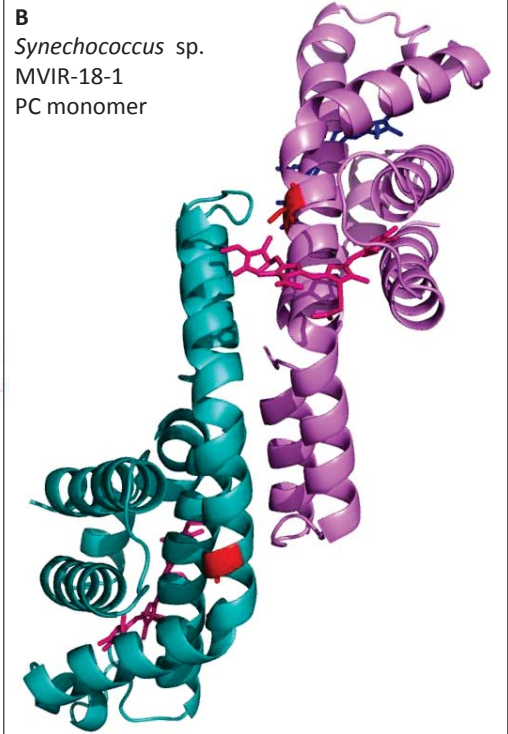
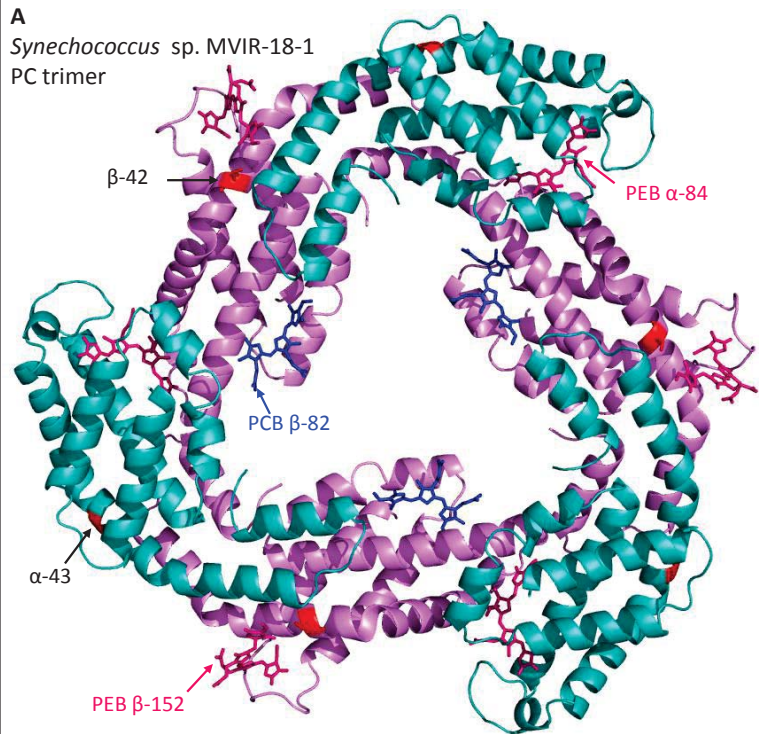












1 **Table 1:** Isolation characteristics and growth temperature properties of the six marine *Synechococcus*  
 2 strains used in this study. For more details, see the Roscoff Culture Collection (RCC) website.

Strain name	RS9907	M16.1	WH7803	ROS8604	MVIR-16-2	MVIR-18-1
<b>RCC strain number</b>	2382	791	752	2380	1594	1682
<b>Phylogenetic clade</b> <sup>1</sup>	II	II	V	I	I	I
<b>Isolation area</b>	Red Sea	Gulf of Mexico	Sargasso Sea	English Channel	Southern Norway Sea	Southern Norway Sea
<b>Isolation latitude</b>	29°28' N	27°42' N	33°45' N	48°43' N	60°19' N	61°00' N
<b>Isolation longitude</b>	34°55' E	91°18' W	67°30' W	3°59' W	3°29' W	1°59' E
<b>Mean annual water temperature (°C)</b> <sup>2</sup>	24.1 ± 0.6	25.8 ± 0.3	22.7 ± 0.2	13.6 ± 0.3	10.3 ± 0.2	10.2 ± 0.2
<b>Annual water temperature amplitude (°C)</b> <sup>2</sup>	5.5 ± 0.7	6.9 ± 0.9	5.9 ± 0.5	5.3 ± 0.6	3.1 ± 0.4	4.4 ± 0.4
<b>Temperature range for growth (°C)</b>	18 - >35 <sup>3</sup>	18 - >35 <sup>4</sup>	16 - 34 <sup>4</sup>	16 - 30 <sup>4</sup>	<12 - 25 <sup>4</sup>	<9 - 25 <sup>4</sup>
<b>Optimal growth temperature (°C)</b>	30 – 32 <sup>3</sup>	32 <sup>4</sup>	33 <sup>4</sup>	26 <sup>4</sup>	22 <sup>4</sup>	22 <sup>4</sup>

3 <sup>1</sup> According to Fuller *et al.* (2003), Mazard *et al.* (2012) and Pittera *et al.* (2014) <sup>2</sup> Average temperature and temperature  
 4 amplitude at the strain isolation sites (resolution: 5x5° squares) over the 2004-2014 period, as derived from satellite data  
 5 from the National Oceanic and Atmospheric Administration (NOAA) <sup>3</sup> This study <sup>4</sup> According to Pittera *et al.* (2014).